Inductance Estimation for Square-Shaped Multilayer Planar Windings

Theofilos Papadopoulos, Antonios Antonopoulos
National Technical University of Athens
School of Electrical and Computer Engineering
Zografou, Greece
E-Mail: teopap@mail.ntua.gr

Keywords

«Planar Magnetics», «Planar Transformer», «High-Frequency Transformer», «High Power Density Systems»

Abstract

In this paper the inductance of square-shaped multilayer planar windings (MLPW) for power applications is investigated. Three well-known equations Wheeler's, Rosa's, and Monomial, which are suitable for single-layer (L1) planar windings, are extended to properly appertain to multilayer architectures. The proposed procedure is verified for two-layer (L2) windings, and the extension to three-layers (L3) or more is discussed, for different values of the geometric parameters. Furthermore, the dependance of the coupling factor k with respect to the distance between the layers is investigated for L2. Finally, an experimental verification is carried out, for a number of selected windings.

Introduction

The continuous effort towards miniaturization and high-efficiency systems is bringing passive elements to the foreground, as they are taking up a large portion of the overall volume in state-of-the-art electronic converters. Within this scope, planar windings (PWs) are considered, due to their low profile and suitability for high-frequency applications. PW-based magnetic components have accurately predetermined values of inductance and capacitance, and can be printed directly on a printed circuit board (PCB) [1], lowering the cost of the manufacturing process. Their inherent characteristic of well-known inductance and capacitance values can be utilized in resonant converters (including series-resonant, LLC, CLLC etc.) [2], [3], even in combination with common-mode noise rejection [4], where the exact knowledge of the resonant tank values is of paramount importance for an efficient soft-switching control scheme, over a wide range of operating conditions.

Several equations have been proposed in literature [5], for the estimation of the total inductance of PWs, mainly focusing on square-shaped, single-layer designs of relatively small dimensions [6]. Generalizing the shape or the dimensions is not an easy task, and methods deducing very complex equations using electromagnetic field analysis have been suggested [7], [8]. Another approach is to adapt well-known and relatively simple equations for inductance estimation of PWs, namely Wheeler's (WH) [9], [10], Rosa's (RS) [11], and the Monomial (MN) [10], to different shapes. It has been shown [12] that extending from relatively small, square-shaped to considerably larger, rectangle-shaped windings is possible, with very accurate results.

This study aims for a different extension of the three aforementioned equations to MLPWs, namely for two, three and four layers. The limitations of this extension are discussed, aiming to provide a better understanding of the effect different design factors impose on the characteristics of an MLPW.

Analysis of Planar Winding Design Parameters

The fundamental equations for inductance estimation of PWs under consideration are

$$L_{\text{Wheeler}} = 1.17\mu_0 \mathrm{N}^2 \frac{D+d}{1+2.75\dfrac{D-d}{D+d}}, \tag{1}$$

$$L_{\text{Rosa}} = 0.3175\mu_0 \mathrm{N}^2 (D+d)\left(\ln\left(2.07\frac{D+d}{D-d}\right)+0.18\left(\frac{D-d}{D+d}\right)+0.13\left(\frac{D-d}{D+d}\right)^2\right), \tag{2}$$

$$L_{\text{Monomial}} = 1.62\cdot 10^{-12} N^{1.78} \left(10^6 D\right)^{-1.21} \left(10^6 w\right)^{-0.147} \left(10^6 \frac{D+d}{2}\right)^{2.4} \left(10^6 s\right)^{-0.03}, \tag{3}$$

where D and d are the outer and inner-side lengths, respectively, w is the width of the copper trace, s is the spacing between two adjacent traces and N is the total number of turns, as presented in Fig. 1. Three extra parameters are necessary to be defined for the extension to multiple layers, namely the number of turns per layer N_T, the number of layers N_L, where $N = N_T N_L$, and the distance between two consecutive layers O, as presented in Fig. 2a.

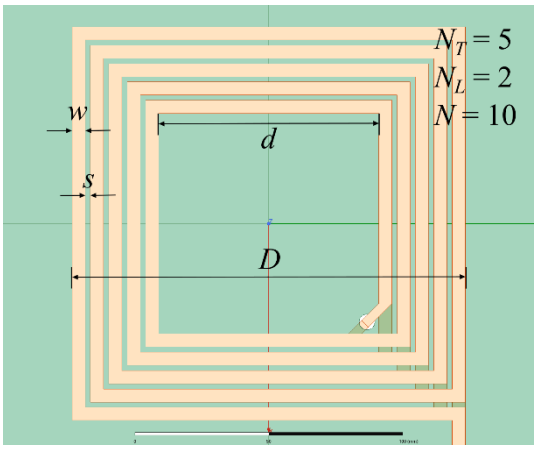

Fig. 1: Two-Layer Planar Winding (L2PW) of $N = N_T N_L$ = 5x2 turns and inner connection, with each parameter D, w, s, d presented.

Several observations can be made about the behavior of the inductance value for L1PWs. The term $(D + d)/2$, which is the average diameter of the square copper ring, is present in all three equations in such a way that the inductance is proportional to it. Eq. (2) also contains the filling factor $(D - d)/(D + d)$ term in the numerator, which is always less or equal to one, multiplied by terms also less than one, which reduces its weight on the final result. This means that large outer and inner sides lead to large inductance values for a given number of turns N. However, for a given voltage and current, w and s are limited by the electrical ratings, and there is no significant room for adjustments. Consequently, the physical dimensions of the board and the number of turns N determine dimensions of the outer and the inner sides, respectively.

To overcome this design limitation and increase the inductance without stretching the physical dimensions significantly, MLPWs are introduced, as a way to increase d for a given D (through shifting some of the turns to different layers), without compromising the nominal power of the winding or changing the total number of turns. Nevertheless, the effect of this action on the estimation of inductance should be addressed in more detail, considering also that a coupling factor is now introduced between the multiple layers. This coupling factor provides an insight on the behavior of the windings in case they are utilized as a high-frequency transformer.

Two indicative schematics of an L2 and an L4PW are presented in Fig. 2, with the distance between the layers exaggerated. The independent design parameters are D, w, s, N_T, N_L, and O. While N_L can be considered indirectly by substituting $N = N_T N_L$ into the aforementioned equations, O is not taken into account, although it is expected to be inversely correlated to the coupling factor, and hence, inversely

correlated to the total inductance. The inner-side length d is a parameter dependent on the rest of the dimensional variables, and can be expressed as a function of the other parameters, as in

$$d = D - 2\frac{N}{N_L}(w+s) + 2s = D - 2N_T(w+s) + 2s\,. \tag{4}$$

For a winding capable of transferring a few tens of kW, the applied voltage is typically up to hundreds of V and the current up to tens of A. According to the IPC-2221 standard, to safely handle these values, the traces should be designed with w from 3 to 5 mm and s from 0.1 to 2 mm, depending on the position of the trace (internal or external PCB layer) and the type of the insulation mask. In this investigation, D is selected to vary from 100 to 210 mm and the number of turns per layer is set to $N_T = 5$, while d can be calculated from (4). It should be noted that when s is one order of magnitude less that w, the term $2\,N_T\,(w + s)$ is much greater from the term $2s$, hence d depends strongly on D and the product $N_T\,(w + s)$. For fixed values of the outer side length and the number of turns, the sum $(w + s)$ determines the inner side, and therefore it strongly influences the total inductance.

All simulations are conducted with Maxwell3D of ANSYS, for an analysis region of 700x700x700 mm^3 and a meshing of around 50 thousand tetrahedras. The excitation current is sinusoidal with 1 A amplitude and a frequency of 100 kHz. The current and frequency are reported for the sake of completeness, since they mainly affect a potential use of a ferrite core in this setup, which this beyond the scope of this study. Furthermore, it was confirmed by simulations that the connection placement between the layers does not affect in any significant manner the total inductance, and can be done either from the inner or the outer side of the winding. Hence, the inter-layer connectors are placed in such a way to minimize their length: at the inner side for L2, at the inner and then outer side for L3, etc.

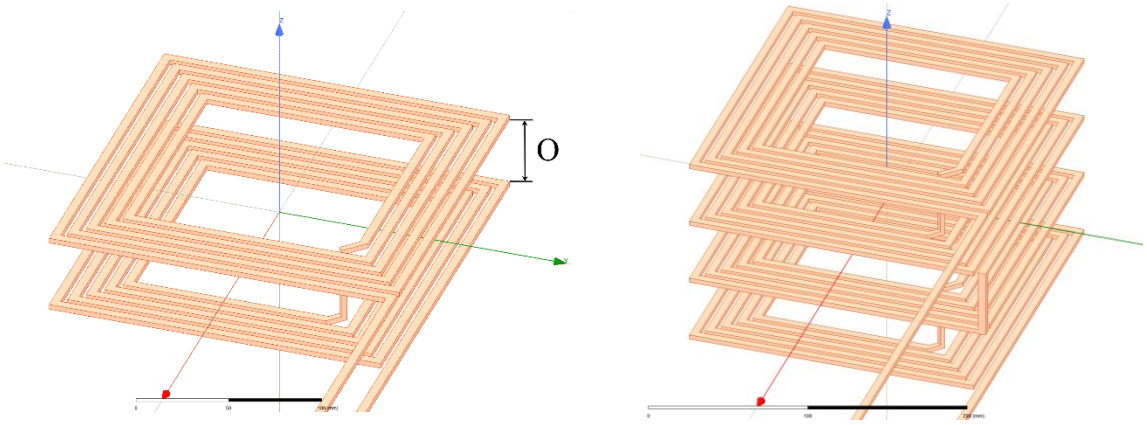

(a) (b)

Fig. 2: Simulated MLPW (a) L2 with inner connection and (b) L4 with inner-outer-inner connection, with the distance between layers exaggerated.

It should be noted that for all simulations, D was varied with a step of 10 mm, resulting in 12 values, w was assigned three values, namely {3, 4, 5} mm, six values were selected for s, namely {0.1, 0.2, 0.5, 0.8, 1.0 2.0} mm, and three values for O, i.e., {0.8, 1.6, 3.2} mm, resulting in 648 simulations for each group (L2, L3, L4) and a total number of 1,944, for all the different combinations of the design dimensions.

Two-Layer Design

Two L1 windings with the same dimensions, connected in series and properly folded, as presented in Fig. 2a, can potentially even quadruple the total inductance, as it is indicated by the N^2 term in the equations. The exact amount of increase in inductance is determined by the coupling factor k, which can be calculated as

$$L_{L2} = 2L_{L1} + 2kL_{L1} \Rightarrow k = \frac{1}{2}\frac{L_{L2}}{L_{L1}} - 1, \tag{5}$$

where L_{L1} is the inductance for the L1PW of N_T turns and L_{L2} is the total inductance for the L2PW of $2N_T$ turns. In this case, k is calculated using the simulation results for L_{L1} and L_{L2}. After simulating the L2PW, with the variance of each parameter described previously, and their corresponding L1PWs, the dependance of k with respect to D and w, for s = 0.5 mm, is presented in Fig. 3a. Accordingly, extracting only the results for a single value of w, i.e., w = 4 mm, the dependence of k and D and s is illustrated in Fig. 3b. Each surface corresponds to a different value of O, namely 0.8 mm, 1.6 mm, and 3.2 mm, from top to bottom.

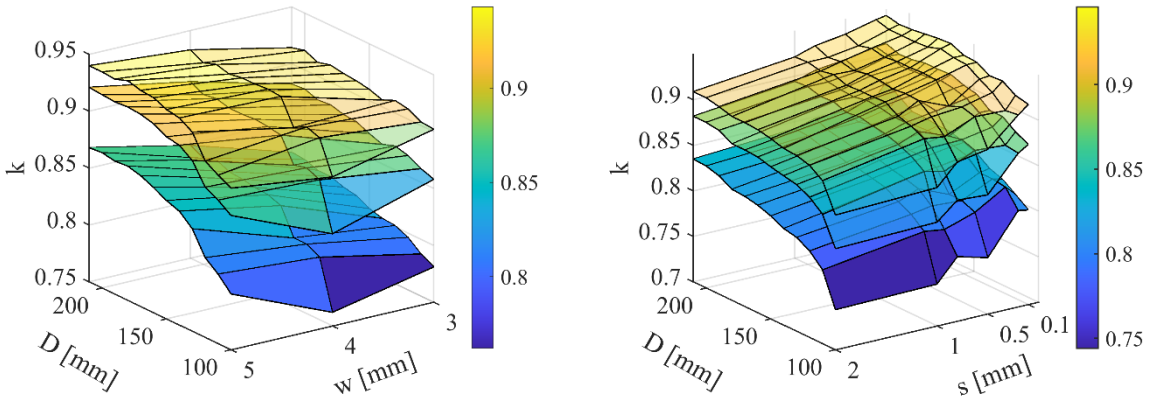

Fig. 3: For fixed number of turns N = 10 and O = {0.8, 1.6, 3.2} mm (top to bottom), the coupling coefficient k, as a function of (a) D and w, for constant s = 0.5 mm, and (b) D and s, for constant w = 4 mm

As it is expected, k is inversely correlated to O, since less of the magnetic flux generated by each layer passes through the other, when O increases. Although O can be arbitrarily large (e.g., up to a few centimeters in wireless power transfer setups), the minimum allowable value is determined by the voltage difference of the vertically separated tracks and the dielectric properties of the insulating material (e.g., FR4). Another interesting observation is that k significantly increases with D. Regarding the other two parameters, k seems to increase with w and decrease with s. These effects are, however, minor compared to D. For this coreless case study, the coupling factor varies from 0.75 for O = 3.2 mm, s = 2 mm, w = 3 mm, and D = 100 mm, to 0.95 for O = 0.8 mm, s = 0.1 mm, w = 5 mm, and D = 210 mm.

The resulting simulated inductances, for a fixed number of $N_T N_L$ = 5x2 = 10 turns, vary from 9 μH to 45 μH and depend strongly on D, with w and s having low impact on their values, as it can be observed in Fig. 4. Even though the coupling factor between two windings tends to increase with w, the total inductance of the winding decreases, since d becomes smaller (for the same D). Similarly, as s increases, both d and k decrease, and the total inductance follows the same trend too. The three surfaces in each subfigure of Fig. 4 correspond to O = {0.8, 1.6, 3.2} mm (from top to bottom), and are very close to each other, with less than 5% difference for the same D, w, and s. This shows that a vertical separation of the layers in the range of up to 3.2 mm has very little impact on the total inductance of the winding. In order to observe large differences, it is mandatory to make O significantly larger, which in the context of MLPW, is not practical, but would still be relevant for WPT setups.

In Fig. 5 the Mean Absolute Errors (MAEs) between the estimations from (1) – (3) and the respective simulation results are presented, to show the accuracy of the equations, with respect to w and s. Each of the MAE% points represent the Mean Absolute Error % among a set of different D values (from 100 to 210 mm). It can be observed that for O = 0.8 mm, the equations provide accurate results, with MAE always less than 4%. In the worst case, for O = 3.2 mm, (1) and (2) provide an increased, albeit accepta-

ble, MAE of less than 8% and 9%, respectively. Furthermore, the MAE created by these two approximations, increases with *s,* and decreases with *w*. This behavior is mainly attributed to the fact that the two equations relate to the current sheet approximation, and provide better results as the copper ring (sheet) becomes larger (i.e., larger *D*) and more dense (i.e., smaller *s*, larger *w*). The MAE of the Monomial approximation does not present a monotonic behavior, but it is also acceptable, as it is less than 6% in any case.

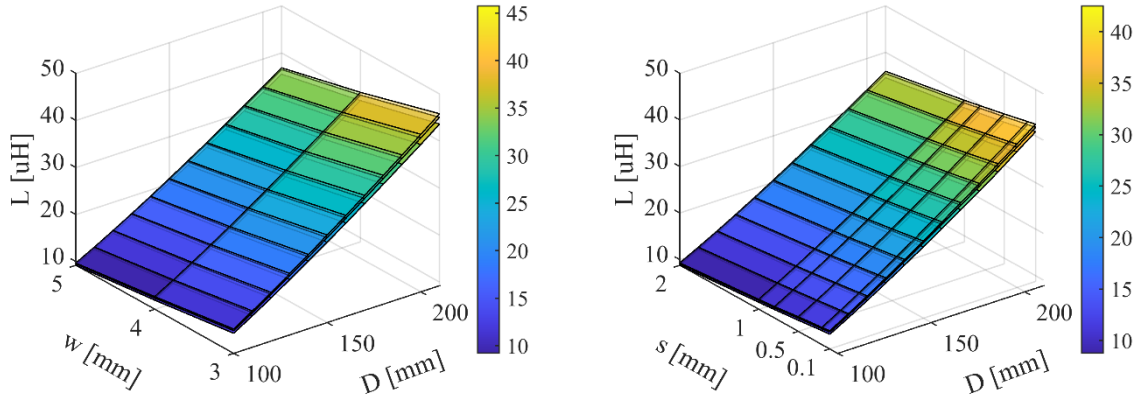

Fig. 4: For fixed number of turns $N = 10$ and $O = \{0.8, 1.6, 3.2\}$ (top to bottom) (a) the total inductance, as a function of D and w, for constant $s = 0.5$ mm, and (b) the total inductance, as a function of D and s, for a constant $w = 4$ mm.

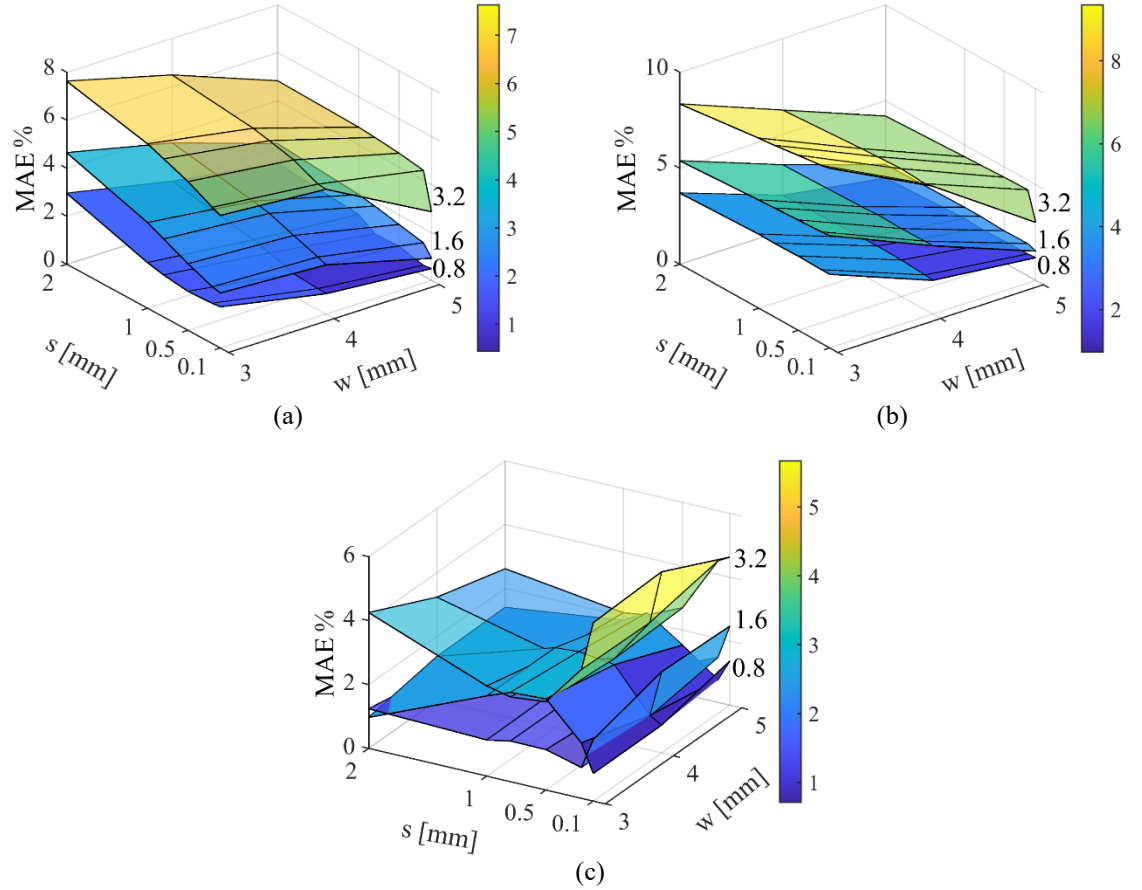

Fig. 5: MAE % for L2 and a fixed number of turns $N = N_T\, N_L = 10$ and $O = \{0.8, 1.6, 3.2\}$ (bottom to up), as a function of *s* and *w,* for (a) Wheeler's, (b) Rosa's and (c) the Monomial equations.

It should be noted that (1) and (2), in most L2 cases, provide an inductance estimation that is larger compared to (3), as can be seen in the Appendix for a selected number of windings. As these equations do not account for the effect of the coupling factor, it is reasonable to expect an overestimation of L, and therefore, increased MAE from (1) and (2) as O increases. In contrast, (3) presents a non-monotonic behavior. This behavioral difference can be mainly attributed to two reasons: In the first place, while (1) and (2) contain the N^2 term, the corresponding term in (3) is only $N^{1.78}$. This means that the inductance value resulting from (3) tends to increase less with each additional turn, compensating for the (less that one) coupling factor in multilayer architectures. This effect is pronounced especially in the cases of large vertical distances between the layers, e.g., for $O = 3.2$ mm. Additionally, (1) and (2) consider the average diameter $(D+d)/2$ raised to the power of one, and the filling factor $(D-d)/(D+d)$, raised to different power values. On the contrary, (3) does not consider the filling factor at all, and raises the average diameter to the power of 2.4. At the same time, the outer diameter D is raised to -1.21. This can also explain the non-monotonic behavior of the MAE when using (3). Due to these observations, it can be assumed that the Monomial equation, as expressed in (3), can provide a more accurate estimation of inductance in the case of MLPWs, especially as O increases.

Three- and Four-Layer Designs

Introducing more layers, with the proper orientation and inter-layer connections, results to windings with $N_T N_L$ turns, while the central aperture remains the same, with an area of d^2. The corresponding increase in the z-axis is negligible, since each new layer increases the profile by only a few mm. This leads to windings with exponentially higher inductance, as it has been discussed in the previous section.

The magnetic interaction between each layer defines three coupling factors, which can be calculated as in the L2 case, but their exact values do not contribute much to the analysis. It can be expected that the mutual flux linkage between any two layers follows the same trend as before and reduces as O increases. This means that, for example the middle layer in an L3 design presents higher inductance compared to the two outer layers, and hence experiences a greater voltage drop. This behavior shall be kept under consideration when the vertical distance of the layers is close to the breakdown voltage of dielectric material.

The resulting simulated inductances for different L3 design cases are presented in Fig. 6, with respect to D and w, for $s = 0.5$ mm and with respect to D and s, for $w = 4$ mm. As in the L2 cases, the inductance is strongly dependent and increases with D, while decreases with w and s but with a weaker dependence on these factors. In order to show that the relation of the N^2 term still holds, the resulting inductance of two designs with the same dimensions in L2 and L3 forms are compared. For $D = 100$ mm, $w = 5$ mm, $s = 1$ mm, and $O = 1.6$ mm, the inductance of the L2 case is 8.714 μH, while for the same dimensions the L3 case winding presents an inductance of 19.178 μH, which is approximately $(15/10)^2 = 2.25$ times more, confirming the N^2 term, at least when O is small enough.

The MAE between simulation and approximated results for the L3 designs for each of the three equations, with respect to w and s, with D varying from 100 mm to 210 mm, is presented in Fig. 7. As it is expected from the L2 case, the MAE increases with O for (1) and (2), resulting in inaccurate values for $O = 3.2$ mm (more than 10% off the simulated ones). The Monomial approximation, on the other hand, continues to provide accurate approximations (below 10% off the simulated values in all cases). It is interesting to observe that the correlation of the approximation accuracy to the vertical separation O is the opposite compared to the other two approximating equations, providing smaller errors when the vertical separation increases. This effect is the result of the inductance underestimation (attributed to $N^{1.78}$) as it was discussed previously.

Considering the N^2 relation to the inductance, it is easy to confirm that it holds by adding another layer to the design example discussed previously ($D = 100$ mm, $w = 5$ mm, $s = 1$ mm, $O = 1.6$ mm). The simulated inductance for the L4 design is 32.972 μH, which is 3.78 times larger from the L2 corresponding winding, hence, slightly smaller from the expected ratio of $(20/10)^2 = 4$. Studying the MAE for the results of each approximating formula in the L4 case, (1) and (2) provide relatively accurate results for

O = 0.8 mm, but exceed the 10% in MAE for higher O values, as can be seen in Fig. 8. In contrast, the $N^{1.78}$ term in (3) compensates the increase of the stray inductance in ML designs, providing very accurate results, with less than 8% MAE for the worst case. The inverse correlation to the increasing vertical spacing O can be stressed once again, according to the resulting MAE shown in Fig. 8c.

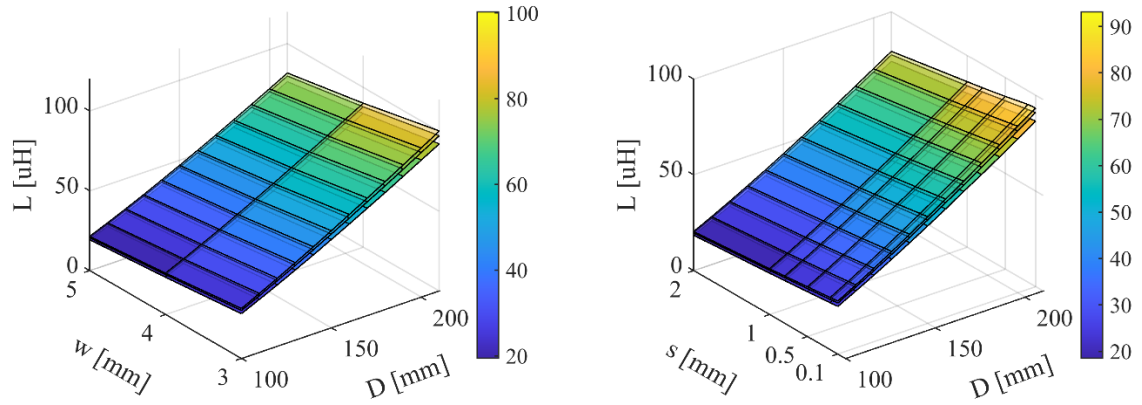

Fig. 6: For L3, with a fixed number of turns N = 15 and O = {0.8, 1.6, 3.2} mm (top to bottom) (a) the total inductance, as a function of D and w, for constant s = 0.5 mm, and (b) the total inductance, as a function of D and s, for a constant w = 4 mm.

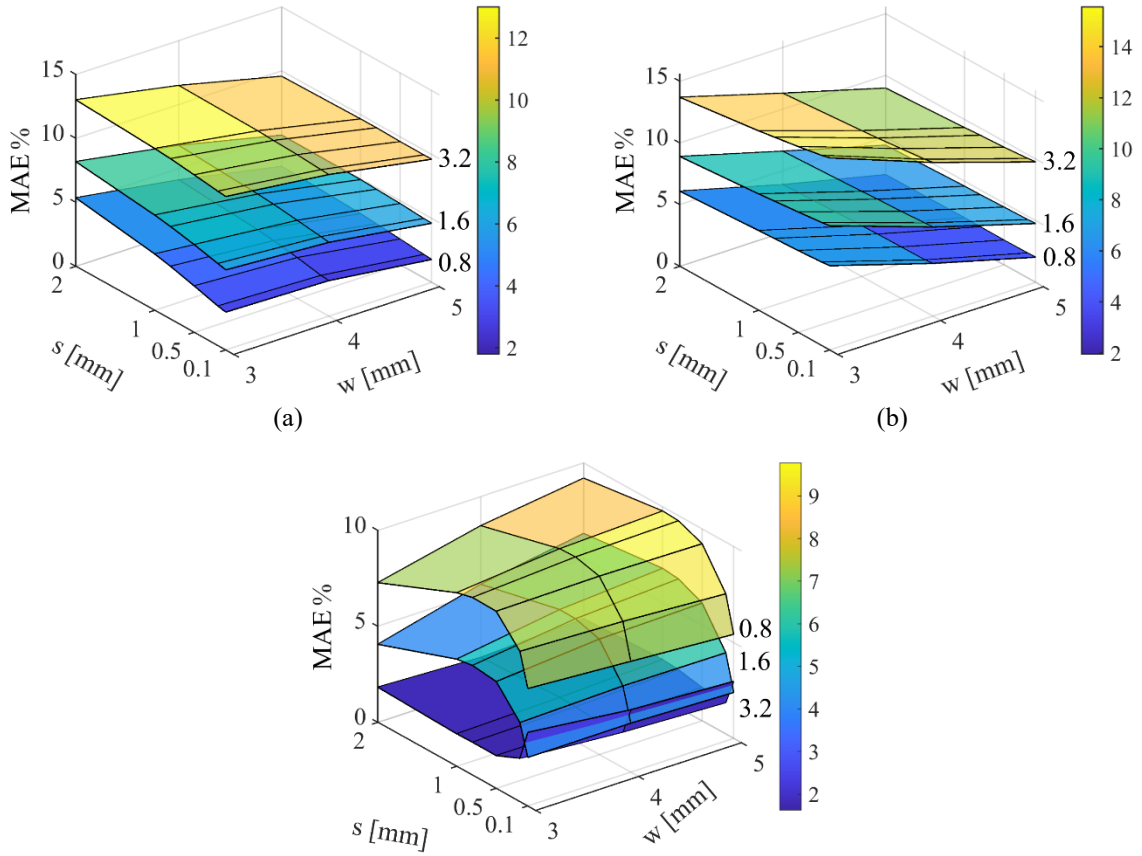

Fig. 7: MAE % for L3 and a fixed number of turns $N = N_T N_L$ = 15 and O = {0.8, 1.6, 3.2} mm for (a) Wheeler's, (b) Rosa's and (c) the Monomial equations.

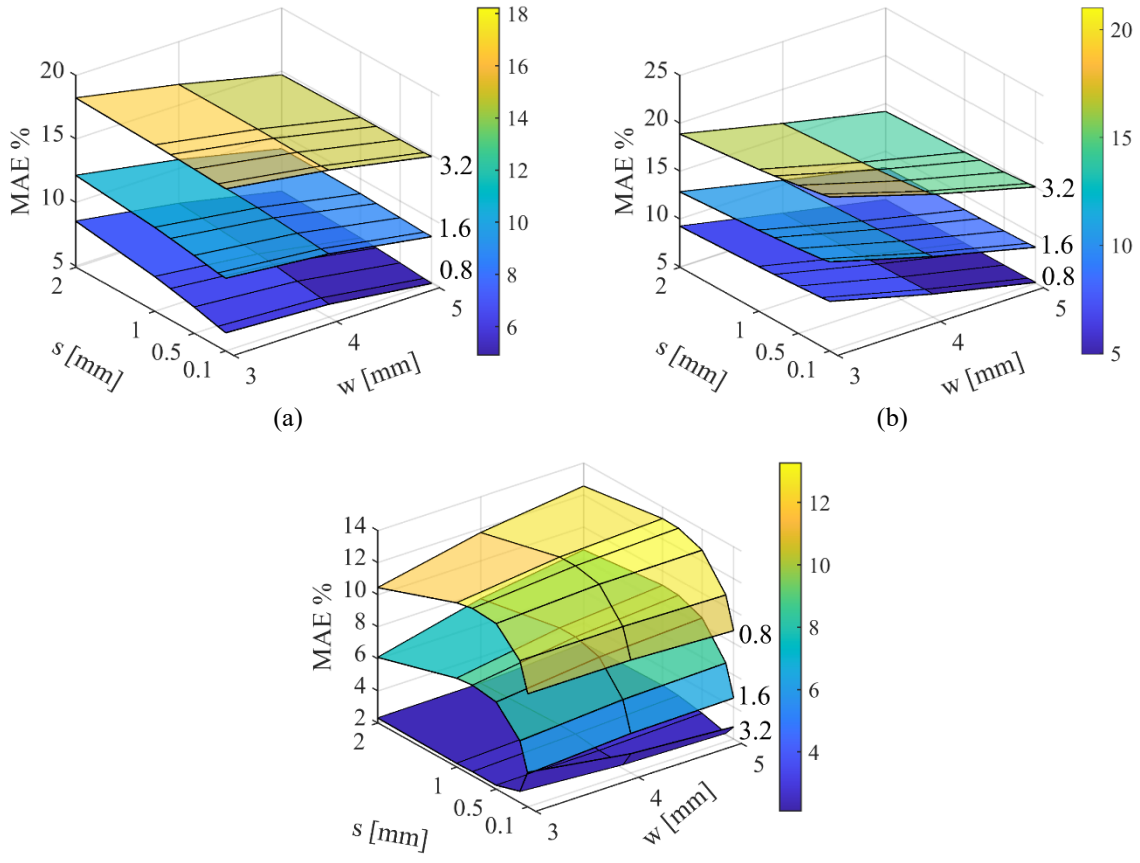

Fig. 8: MAE % for L4 and a fixed number of turns $N = N_T N_L = 20$ and $O = \{0.8, 1.6, 3.2\}$mm for (a) Wheeler's, (b) Rosa's and (c) the Monomial equations.

The estimation of inductance for windings with five layers or more cannot rely on (1) and (2), since the errors become unacceptable. Better estimations can be provided by (3), especially for cases with significant vertical separation between consecutive windings. For design cases with more than 5 layers the need for new estimation equations, which take into account O, can be considered.

Experimental Results

In order to verify the accuracy of both the equations and the simulation results, six MLPW have been printed and tested in the laboratory. The tests were conducted using a modified power amplifier for frequency, voltage, and current up to 50 kHz, 30 V and 2 A, respectively. In Fig. 9 the laboratory setup and one indicative case of an L2PW are illustrated. The results are presented in Table I, where the inductance is measured for 50 kHz, and is in good agreement, with less than 2.5 % error between the simulated and measured inductances. The error between each equation and measurement is presented in the three last columns, for Wheeler's, Rosa's, and the Monomial, respectively. It is less than 10% in any case, and less than 5% for the vast majority of the samples.

Considering the N^2 relation to the inductance, its validity can be highlighted once again for the MLPW described previously, but in this case from the measured values. The inductance of the L2PW is 8.912 μH, and the corresponding L3 and L4 cases are 19.564 and 33.512 μH, respectively, leading to: (19.564/8.912) = 2.2 ≈ 2.25 and (33.512/8.912) = 3.76 ≈ 4. Also, the reduction of the inductance as O increases (from 1.6 to 3.2 mm) is verified from rows 2 and 3, with a 4.3% reduction. Similarly, rows 4 and 5 indicate a 7.3% reduction. Finally, the strong dependence of inductance on d can be observed when comparing rows 1 and 2: for the same D, and with 2 mm difference (approximately 5%) in d, the inductance is increased by the same percentage, from 8.912 to 9.384 μH.

Table I: Experimental results for six indicative MLPW arrangements

Dimensions [mm]							Equations [μH]					Error %		
N_L	D	w	s	N	d	O	WH	RS	MN	Sim	Meas	WH	RS	MN
2	100	4	2	10	44	1.6	9.377	9.284	9.302	9.202	9.384	-0.07	-1.08	-0.88
2	100	5	1	10	42	1.6	8.788	8.711	8.888	8.714	8.912	-1.41	-2.31	-0.27
2	100	5	1	10	42	3.2				8.485	8.532	2.91	2.05	4.01
3	100	5	1	15	42	1.6	19.774	19.601	18.291	19.178	19.564	1.06	0.19	-6.96
3	100	5	1	15	42	3.2				17.927	18.125	8.34	7.53	0.91
4	100	5	1	20	42	1.6	35.153	34.846	30.523	32.972	33.512	4.67	3.83	-9.79

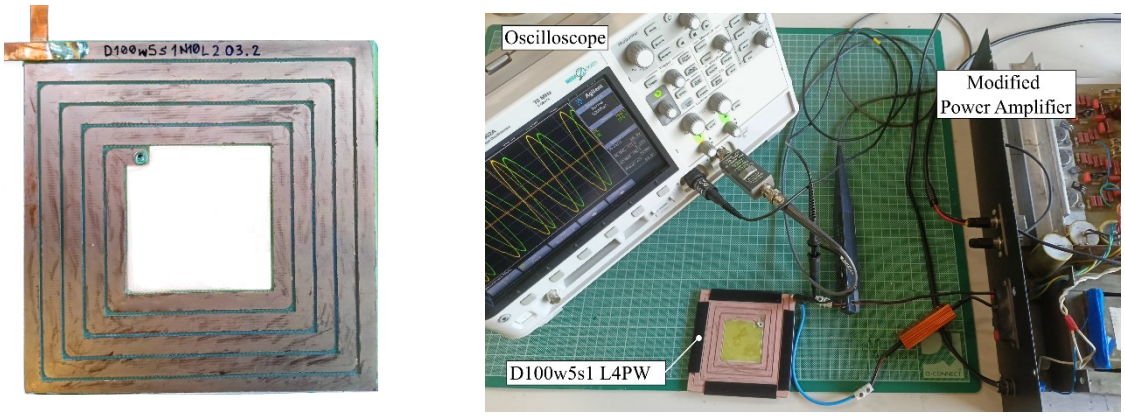

(a) (b)

Fig. 9: (a) An indicative case of L2PW with D = 100 mm, w = 4 mm, s = 2 mm and O = 1.6 mm, and (b) the experimental setup for impedance and inductance measurement.

Conclusion

In this study, an effort to estimate the inductance for square-shaped MLPW has been made, using well-established approximation equations for L1 counterparts. A large number of MLPW have been simulated, with a variety of design dimensions (D, d, w, s, O, N_T, N_L), to quantify the accuracy of these approximations and its dependence on the number of layers and the vertical spacing between them. For the L2 case, all equations provide an acceptable level of accuracy, with less than 9% MAE, up to a reasonable O = 3.2 mm. The coupling factor in this case is relatively high, even without utilization of a ferrite core. For the L3 case, the Monomial provides accurate results, with less than 9% MAE for all values of O, while Wheeler's and Rosa's equations can be trusted only when layers are vertically close, with less than 1.6 mm spacing. For L4 designs, the accuracy of Wheeler's and Rosa's approximations is limited to small values of O, while the Monomial can still approximate relatively accurately, especially with increasing vertical separation.

References

[1] C. Buttay *et al.*, "Application of the PCB-Embedding Technology in Power Electronics-State of the Art and Proposed Development," *3D-PEIM 2018 - 2nd Int. Symp. 3D Power Electron. Integr. Manuf.*, 2018, doi: 10.1109/3DPEIM.2018.8525236.

[2] Y. C. Liu *et al.*, "Design and implementation of an integrated planar transformer for high-frequency LLC resonant converters," *Conf. Proc. - IEEE Appl. Power Electron. Conf. Expo. - APEC*, vol. 36, no. 5, pp. 2883–2890, 2021, doi: 10.1109/APEC42165.2021.9487046.

[3] Z. Zhang, C. Liu, M. Wang, Y. Si, Y. Liu, and Q. Lei, "High-Efficiency High-Power-Density CLLC Resonant Converter with Low-Stray-Capacitance and Well-Heat-Dissipated Planar Transformer for EV On-Board Charger," *IEEE Trans. Power Electron.*, vol. 35, no. 10, pp. 10831–10851, 2020, doi: 10.1109/TPEL.2020.2980313.

[4] K. W. Kim, Y. Jeong, J. S. Kim, and G. W. Moon, "Low Common-Mode Noise LLC Resonant

Converter with Static-Point-Connected Transformer," *IEEE Trans. Power Electron.*, vol. 36, no. 1, pp. 401–408, 2021, doi: 10.1109/TPEL.2020.3004168.
[5] M. K. Kazimierczuk, *High-Frequency Magnetic Components*. John Wiley & Sons, Ltd, 2014.
[6] A. M. Niknejad and R. G. Meyer, "Analysis, design, and optimization of spiral inductors and transformers for Si RF Ie's," *Phase-Locking High-Performance Syst. From Devices to Archit.*, vol. 33, no. 10, pp. 89–100, 2003, doi: 10.1109/9780470545492.ch8.
[7] H. A. Aebischer, "Inductance formula for rectangular planar spiral inductors with rectangular conductor cross section," *Adv. Electromagn.*, vol. 9, no. 1, pp. 1–18, 2020, doi: 10.7716/aem.v9i1.1346.
[8] C. Peters and Y. Manoli, "Inductance calculation of planar multi-layer and multi-wire coils: An analytical approach," *Sensors Actuators, A Phys.*, vol. 145–146, no. 1–2, pp. 394–404, 2008, doi: 10.1016/j.sna.2007.11.003.
[9] H. A. Wheeler, "Simple inductance formulas for radio coils," *Proc. Inst. Radio Eng.*, vol. 16, no. 10, pp. 1398–1400, 1928, doi: 10.1109/JRPROC.1928.221309.
[10] S. S. Mohan, M. D. M. Hershenson, S. P. Boyd, and T. H. Lee, "Simple accurate expressions for planar spiral inductances," *IEEE J. Solid-State Circuits*, vol. 34, no. 10, pp. 1419–1420, 1999, doi: 10.1109/4.792620.
[11] E. B. Rosa and F. W. Grover, "Formulas and tables for the calculation of mutual and self-inductance (Revised)," *Bull. Bur. Stand.*, vol. 8, no. 1, p. 1, 1912, doi: 10.6028/bulletin.185.
[12] T. Papadopoulos and A. Antonopoulos, "Formula Evaluation and Voltage Distribution of Planar Transformers Using Rectangular Windings," *2021 23rd Eur. Conf. Power Electron. Appl. EPE 2021 ECCE Eur.*, pp. 1–10, 2021.

APPENDIX

Table A: Inductance estimations of the three formulas, for an indicative number of L2 windings.

D	*w*	*N*	*s*	WH	RS	MN	*s*	WH	RS	MN
100	5.0	10	2.0	7.400	7.376	7.574	1.0	8.788	8.711	8.888
110	5.0	10	2.0	9.366	9.293	9.424	1.0	10.905	10.786	10.865
120	5.0	10	2.0	11.446	11.328	11.370	1.0	13.121	12.971	12.932
130	5.0	10	2.0	13.619	13.465	13.400	1.0	15.420	15.251	15.075
140	5.0	10	2.0	15.872	15.691	15.504	1.0	17.787	17.616	17.287
150	5.0	10	2.0	18.193	17.998	17.673	1.0	20.213	20.058	19.561
160	5.0	10	2.0	20.572	20.378	19.901	1.0	22.690	22.571	21.889
170	5.0	10	2.0	23.002	22.825	22.183	1.0	25.209	25.147	24.269
180	5.0	10	2.0	25.475	25.333	24.514	1.0	27.765	27.783	26.695
190	5.0	10	2.0	27.987	27.898	26.891	1.0	30.355	30.474	29.165
200	5.0	10	2.0	30.533	30.517	29.310	1.0	32.972	33.217	31.675
210	5.0	10	2.0	33.109	33.185	31.768	1.0	35.615	36.008	34.222
100	4.0	10	0.5	11.972	11.843	11.751	0.2	12.560	12.436	12.529
110	4.0	10	0.5	14.359	14.233	13.987	0.2	14.990	14.884	14.852
120	4.0	10	0.5	16.817	16.720	16.300	0.2	17.487	17.428	17.250
130	4.0	10	0.5	19.334	19.293	18.681	0.2	20.039	20.056	19.717
140	4.0	10	0.5	21.900	21.944	21.123	0.2	22.636	22.761	22.245
150	4.0	10	0.5	24.506	24.666	23.620	0.2	25.270	25.536	24.828
160	4.0	10	0.5	27.147	27.453	26.168	0.2	27.937	28.375	27.462
170	4.0	10	0.5	29.817	30.299	28.763	0.2	30.630	31.274	30.143
180	4.0	10	0.5	32.512	33.202	31.401	0.2	33.347	34.228	32.867
190	4.0	10	0.5	35.229	36.157	34.080	0.2	36.084	37.233	35.633
200	4.0	10	0.5	37.965	39.160	36.796	0.2	38.838	40.288	38.437
210	4.0	10	0.5	40.718	42.210	39.549	0.2	41.608	43.387	41.277